Journal of the Korean Association for Shell and Spatial Structures
Vol. 4, No. 4 (통권 14호), pp. 65~76, December, 2004

Application of Equivalent Walking Loads for Efficient Analysis of Floor Vibration Induced by Walking

김 기 철* 김 재 열**
Gee-Cheol Kim Jae-Yeol Kim

Abstract

Walking loads are usually considered as nodal loads in the finite element vibration analysis of structures subjected to walking loads. Since most of the walking loads act on elements not nodes, the walking loads applied on the elements should be converted to the equivalent nodal walking loads. This paper begins with measuring walking loads by using a force plate equipped with load cells and investigates the characteristics of the walking loads with various walking rates. It is found that the walking loads are more affected by walking rates than other parameters such as pedestrian weight, type of footwear, surface condition of floor etc. The measured walking loads are used as input loads for a finite element model of walking induced vibration. Finally, this paper proposes the equivalent nodal walking loads that are converted from the walking loads acting on elements based on finite element shape functions. And the proposed equivalent walking loads are proved to be applicable for efficient analysis of floor vibration induced by walking loads.

Keywords: walking load; equivalent walking loads; walking rate; floor system; floor vibration

1. Introduction

Recently, building structures with large open spaces have low inherent damping due to decline in the use of non-structural members such as curtain walls. Furthermore, high-strength material and efficient structural scheme lead to longer spans and more flexible floor systems. Structures with low damping and lightweight have a higher possibility of experiencing excessive vibrations than those of heavy type construction. These excessive vibrations make occupants uncomfortable and raise serviceability problem in buildings. Long span structures with low natural frequencies such as shopping malls, large offices and assembly rooms may experience signification dynamic responses due to human activities such as walking, jumping and stamping. It is now widely accepted that walking load is a major source of floor vibration disturbance. For many years, assessment of serviceability of building structures subjected to walking loads and parametric studies about walking loads have been the majority of research work. But the application of walking loads into the vibration analysis using finite element packages is rarely studied. It is in general that walking loads are treated as nodal loads for finite element vibration analysis of structures. This method requires a large number of nodes and mesh models corresponding to walking strides. Since most of them act on elements not nodes, it is needed to propose new application method of walking loads that are applied on the elements.

In this research, walking loads are directly

* Dept. of Architectural Eng., Seoil College, #49-3, Myoenmok-dong, Jungrang-gu, Seoul, Korea
** Dept. of Architectural Eng., Hyupsung University, Sangri, Bongdam-Eup, Hwasung-Si, Kyunggi-Do, Korea

measured by using a force plate in which two load cells are equipped. Walking loads with various walking rates are measured to analyze the dynamic loads-time traces. And heel drop tests are conducted to obtain the dynamic characteristics of the actual floor system such as natural frequency and damping ratio. The experimentally measured responses under pedestrian walking excitation and the corresponding analytical responses are compared to verify the validity of equivalent walking loads proposed in this paper. The objective of this paper is to propose a new application method of walking loads that are converted from the loads acting on elements based on finite element shape functions for an efficient analysis of floor vibration induced by walking loads.

2. Application of Walking Loads for Vibration Analysis

2.1 Mesh division and master node selection for efficient vibration analysis

It is known that the floor slab should be divided into more than four elements along each side to obtain a relatively accurate response [1]. And the use of square mesh produces a more desirable result [2]. It is required that the master node should be selected properly and the floor slab should be divided appropriately in order to reduce the DOFs. If the floor mesh is refined, the elements and nodal points are increased and much more computer memories are required in numerical analysis. If the mesh division is not carried out adequately along each side, the mode shapes are not represented sufficiently and accurate responses can not be obtained. Therefore, it is very important to divide the analytical model into the appropriate number of elements.

2.2 Application of a series of nodal walking loads

One of the methods to apply walking loads for vibration analysis is to use a series of nodal loads with assigned time delays [5]. This method accounts for the moving effect of walking. It is assumed that a series of nodal loads is applied not to the elements but to the nodes. As shown in Fig. 1, the floor system should be divided into many finite elements according to stride length. Then nodal walking loads with an assigned time delay are applied sequentially at the nodes of the finite elements model for vibration analysis of the floor subjected to walking loads. The assigned time delay is expressed as the difference between the time one foot contacts a point and the other foot contacting an adjacent point. As shown in Fig. 2, a series of nodal walking loads applied at nodes is overlapped because one of the feet is always in contacts with the floor at a given time. The overlap time is represented by subtraction of the

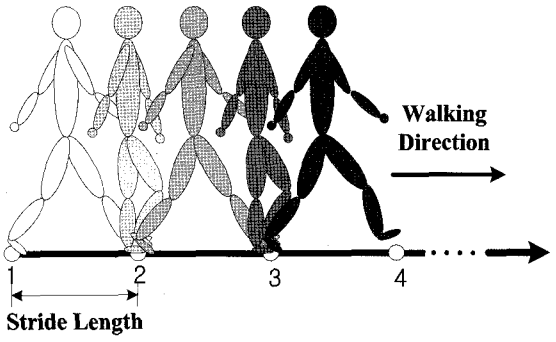

〈Fig. 1〉 Footsteps at nodes

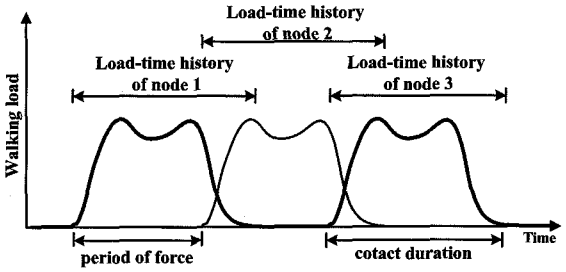

〈Fig. 2〉 Series of walking loads

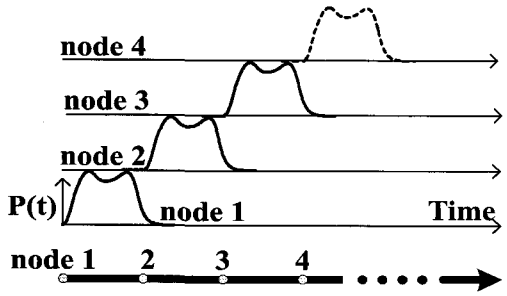

〈Fig. 3〉 Application of a series of nodal walking loads

force period from the contact duration. It is known that the contact duration and the overlap time decrease when the walking rate is higher [3].

As shown in Fig. 3, the nodes are needed as many as the number of strides for the application of a series of nodal walking loads. The series of nodal walking loads have difficulty in being applied as input loads for finite element analysis, because the nodal points should be located at the positions where the footsteps are contacted. If the stride length is changed or the walking load is not applied to the node, the finite element model should be modified. Therefore, a series of nodal walking loads is not effective in the vibration analysis of structures subjected to walking loads.

2.3 Application of equivalent walking loads on beam elements

2.3.1 Conversion of point loads on beam elements

Point loads on beam elements can be replaced by equivalent nodal loads through the use of shape functions for the beam elements as shown in Fig. 4 [6], [7]. Since the beam element has a vertical translational DOF and a rotational DOF at each node, the point load $W(t)$ on the beam element could be represented as the vertical force components (P_i, P_j) and rotational moment

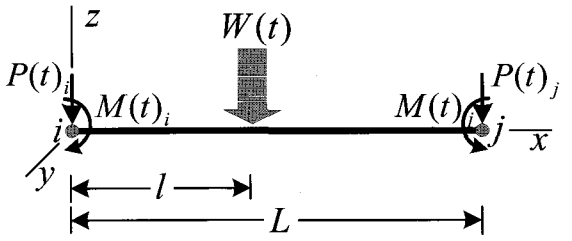

〈Fig. 4〉 Equivalent nodal loads of beam element

components (M_i, M_j) as follows:

$$\begin{bmatrix} P_i(t) \\ M_i(t) \\ P_j(t) \\ M_j(t) \end{bmatrix} = W(t)[f_1 \ f_2 \ f_4]^T \quad (1)$$

where $W(t)$ is the point load and f_1, f_2, f_3 and f_4 are shape functions of the beam element.

Substituting the shape functions in Eq. (1) leads to

$$P_i(t) = W(t)(L-l)^2(L+2L)/(L^3) \quad (2)$$

$$M_i(t) = -W(t)\, l(L-l)^2/L^2 \quad (3)$$

$$P_j(t) = W(t)(L)^2(3L-2l)/(L^3) \quad (4)$$

$$M_j(t) = W(t)\, l(L-l)l^2/L^2 \quad (5)$$

2.3.2 Static analysis of beam model with equivalent nodal loads

Static analysis for the two types of beam models is carried out in order to verify the validity of the equivalent nodal loads. The fixed beam model is 900cm long. Model A is divided into 7 elements and Model B is divided into 14 elements as shown in Fig. 5. The load cases are shown in Table 1. Load case 1 and Load case 2 are equivalent nodal loads without moment loads and with moment loads, respectively. And Load case 3 is nodal point loads on the beam element. Load case 1 and Load case 2 are applied to Model A and Load case 3 is applied to Model B.

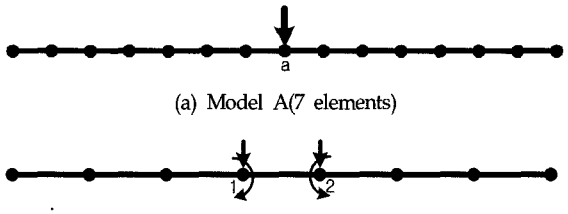

(a) Model A(7 elements)

(b)Model C(14 elements)

〈Fig. 5〉 Beam models

Table 1. Load cases of beam model

Model	Model A		Model B
Load case	Load case1	Load case2	Load case3
Loading Point	1,2	1,2	a
Load	P_i	P_i, M_i	P
	250kg	250kg, ±650kg·cm	500kg

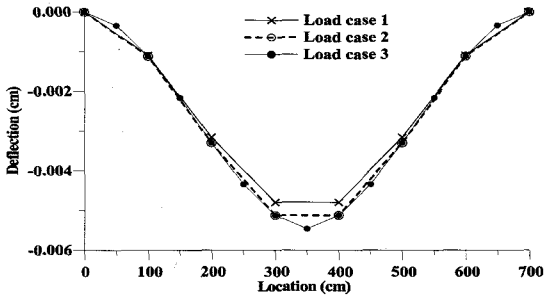

〈Fig. 6〉 Static deflection of beam models

Fig. 6 shows the deflections of beam models corresponding to the three types of load cases. The deflections of Load case 1 are smaller than those of Load case 2 and Load case 3, because moment loads have not been considered in the equivalent nodal loads of Load case 1. There is little difference in the deflections between Load case 2 and Load case 3. Therefore, equivalent walking loads of the beam element are applicable for vibration analysis of beam system subjected to walking loads as shown in Fig. 7.

2.4 Application of equivalent walking loads on plate elements

2.4.1 Conversion of walking loads on plate elements

The MZC rectangle (plate bending element),

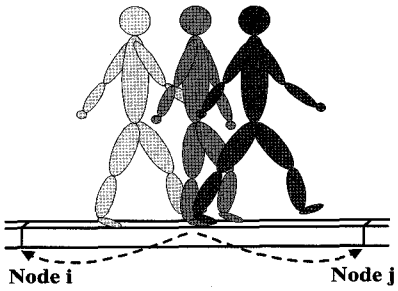

〈Fig. 7〉 Conversion of walking loads on the beam element

which is developed by Melosh, Zienkievicz and Cheung, has only one generic translational displacement(w) in the z direction [4]. The nodal displacements are composed of one vertical displacement and two rotational dis- placements. The displacement function for the MZC rectangle is given in the following expression:

$$w = c_1 + c_2\xi + c_3\eta + c_4\xi^2 + c_{5zi}\eta + c_6\eta^2 + c_7\xi^3 \\ c_8 zi^2\eta + c_9 zi\eta^2 + c^3_{10\eta} + c^3_{11zi}\eta + c_{12}\xi\eta^3 \quad (6)$$

where ξ and η are dimensionless centroidal coordinates as shown in Fig. 8.

The plate bending element has one vertical translational DOF and two rotational DOFs at each node. The shape function satisfying the vertical displacement (w_i), the x-axis rotational displacement ($\partial w_i/\partial x$)and the y- axis rotational displacement($\partial w_i/\partial y$)at node i can be expressed as follows, respectively:

$$f_{i1} = (1/8)(1+\xi_0)(1+\eta_0)(2+\xi_0+\eta_0-\xi^2-\eta^2) \quad (7)$$

$$f_{i2} = (-1/8)b\eta_i(1+\xi_0)(1-\eta_0)(1+\eta_0)^2 \quad (8)$$

$$f_{i3} = (1/8)a\xi_i(1-\xi_0)(1+\eta_0)(1+\eta_0)^2 \quad (9)$$

where $\xi_0 = \xi_i\xi$ and $\eta_0 = \eta_i\eta$,(i =1,2,3,4) and the parameters ξ_i and η_i pertaining to the corners of the rectangle are the generalized nodal coordinates for MZC rectangle elements as shown in

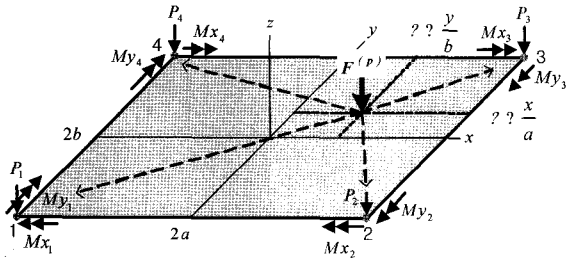

〈Fig. 8〉 Equivalent nodal loads of plate bending element

Fig. 8 in which a and b are half the width and height, respectively. Point loads on the plate bending element can be represented as equivalent nodal loads by using the shape functions of the plate bending element. As shown in Fig. 8, point loads($W(t)$)on the plate- bending element could be converted into one vertical force component$P(t)_i$ and two rotational moments components($M_{xi}(t)$, $M_{yi}(t)$) as follows:

$$\begin{bmatrix} P_i(t) \\ M_{xi} \\ M_{yi}(t) \end{bmatrix} = W(t)[f_{i1}\ f_{i2}\ f_{is}]^T \qquad (10)$$

where f_{i1}, f_{i2} and f_{i3} are the shape functions of i node and i is the node number of the plate bending element.

By substituting the shape functions of the plate bending element into Eq. (10), the equivalent nodal loads of the plate bending elements can be expressed as follows:

$$P_i(t) = W(t)(1/8)(1+\xi_0)(1+\eta_0)(2+\xi_0+\eta_0-\xi^2-\eta^2) \qquad (11)$$

$$M_{zi} = W(t)(-1/8)b\eta_i(1+\xi_0)(1-\eta_0)(1+\eta_0)^2 \qquad (12)$$

$$M_{yi} = W(t)(1/8)a\xi_i(1-\xi_0)(1+\eta_0)(1+\eta_0)^2 \qquad (13)$$

2.4.2 Static analysis of plate model with equivalent nodal loads

The clamped plate models of size 900cm x 500cm have been described as two types of mesh division: Model C (9x5) and Model D (18x10) as shown in Fig. 9. The load cases are shown in Table 2. Load case 1 is for equivalent nodal loads without moment loads. Load case 2 is for equivalent nodal loads with moment loads and Load case 3 is for nodal point loads on the plate element. Fig. 9a shows the deflections of the plate models with different mesh division subjected to three types of loads cases. The deflections are plotted along line A. The deflections of Load case 1 are smaller than those of Load case 2 and Load case 3. There is little difference in deflections between Model C under Load case 2 and Model D under Load case 3. It is shown that the deflections of the plate model subjected to Load case 2 of the equivalent nodal load are in a good agreement with those of the plate model subjected to Loads case 3 of point nodal load. Therefore, it is possible to apply equivalent walking loads of the plate bending element for vibration analysis of the floor system subjected to walking loads as shown in Fig. 10.

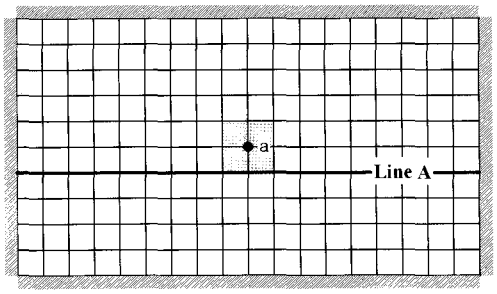

(a) Model A(Mesh 9x5)

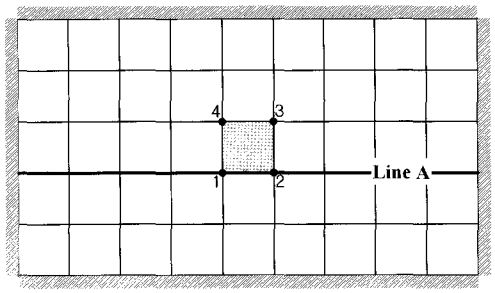

(b) Model B(Mesh 18x10)

〈Fig. 9〉 Plate Models

〈Table 2〉 Load cases of plate model

Model	Model A		Model B
Load case	Load case1	Load case2	Load case3
Loading Point	1,2,3,4	1,2,3,4	a
Load	P_i	P_i, M_{xi},M_{yi}	P
	250kg	250kg, ±650kg·cm	1000kg

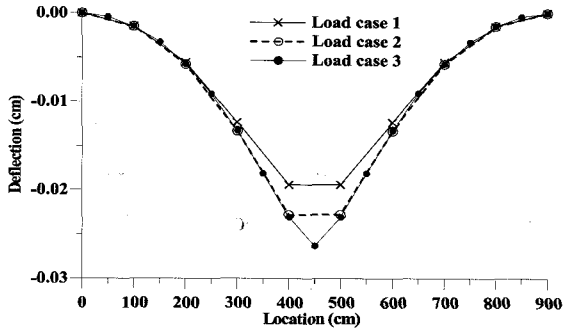

〈Fig. 9a〉 Static deflection of plate models

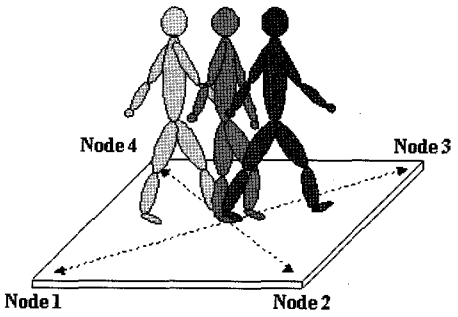

〈Fig. 10〉 Conversion of walking loads on the plate element

3. Vibration Analysis of Structures Subjected to Walking Loads

3.1 Vibration analysis of actual floor system

3.1.1 Dynamic characteristics of actual floor system

For the vibration analysis of an actual floor system, its dynamic characteristics such as damping ratios, vibration modes and natural frequencies are first investigated. Fig. 20 shows the dimensions of the actual concrete floor system

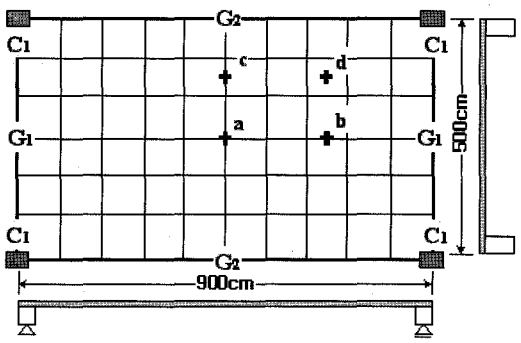

〈Fig. 11〉 Actual floor system

〈Table 3〉 Member size of floor system

Member		Size(cm)
Column	C1	40 x 70
Girder	G1	40 x 75
	G2	40 x 60
Slab		16.5

that is a connection aisle for the pedestrian traffic between the two adjacent building structures. This floor system is simply supported along its edges. The structural member sizes are given in Table 3. Accelerometers for the measuring acceleration responses are placed at point 'a', 'b', 'c' and 'd' as shown in Fig. 11.

The vibration mode shapes and natural frequencies of the actual floor system can be found by analyzing the measured responses at several points. The response spectra of the antinodes, which are the peaks of the vibration mode shape, are greater than those of the other points at the natural frequencies. Fig. 12 shows the first eight mode shapes of the actual floor system obtained by eigenvalue analysis. Point 'a' represents the peaks of the 1st, 4th and 5th mode shapes. The antinode of the 2nd mode shape is point 'b'. Point 'c' is the antinode of the 3rd and 7th mode shapes. And point 'd' is the antinode of the 9th mode shape. Fig. 13(a) shows the response spectrum of the acceleration of point 'a', 'b' and 'd' induced by the heel drop impact loads at point 'a'. The accelerations of point 'a' are more prominent than other points at 19.04Hz,

36.13Hz, 42.48Hz and 67.87Hz that are natural frequencies of the 1st, 4th, 5th and 9th modes respectively, since point 'a' is the peak point of the corresponding mode shapes. Fig. 13 (b) represents the result of spectrum analysis of the accelerations at point 'a', 'b' and 'c' induced by heel drop impact loads at point 'b'. The accelerations of point 'b' are greater than those of the other points at 29.79Hz that is the 2nd natural frequency, because point 'b' is the antinode of the 2nd mode shape. As shown in

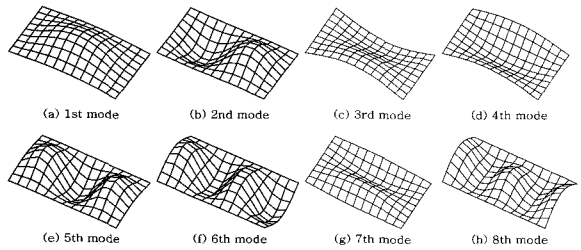

〈Fig. 12〉 Vertical mode shapes of actual floor system

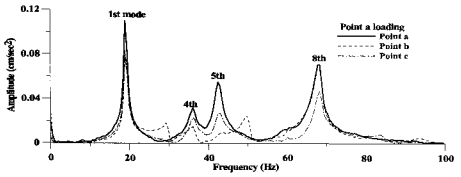

(a) Acceleration response spectrum induced by heel drop at point 'a'

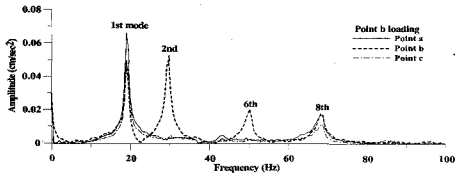

(b) Acceleration response spectrum induced by heel drop at point 'b'

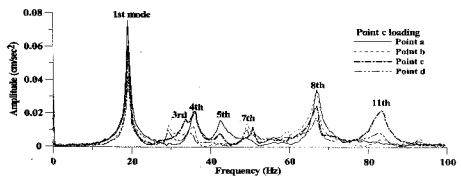

(c) Acceleration response spectrum induced by heel drop at point 'c'

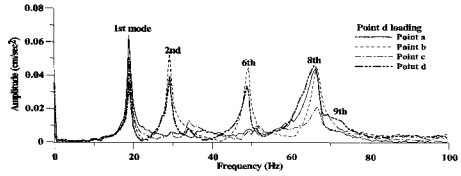

(d) Acceleration response spectrum induced by heel drop at point 'd'

〈Fig. 13〉 Response spectrum of measured acceleration

Fig. 13(c), the responses at point 'c' are more prominent than those of the other points at the 3rd, 4th, 7th and 11th natural frequencies that are 33.69Hz, 36.13Hz, 50.78Hz and 82.52Hz, respectively. The natural frequency of the 8th mode is defined in Fig. 13(d). Natural frequencies of the actual floor system obtained by the heel drop test are compared to those of the analytical model of the actual floor system calculated by the eigenvalue analysis as shown in Table 6 demonstrating that they are in a good agreement. Hence, it means that the stiffness and mass of the analytical model are close enough to those of the actual floor system.

Although damping is the most important parameter in floor vibration, it is very difficult to predict the damping accurately because the type of finishing, concrete weight, plumbing, ceiling and partitions affects the damping of a floor system. Very little research has been conducted to determine the amount of damping contributed by the various components of a completed floor system. Only rough guidelines are available. The Canadian Standards Association suggests the following damping ratio: bare floor-3%, floor finished with ceiling, ducts, flooring and furniture-6%, finished floor with partitions-13%. Damping of the actual floor system is usually characterized by equivalent viscous damping ratios ζ showing a similar decay rate of response under free vibration conditions [9]. The relation between the ratio of two successive peaks of damped free vibration and damping ratio is given by

$$\frac{\ddot{u}_i}{\ddot{u}_{i+1}} = \exp\left(\frac{2\pi\zeta}{\sqrt{(1-\zeta^2)}}\right) \quad (14)$$

where, $\ddot{u}_i$ and $\ddot{u}_{i+1}$ are the consecutive accelerations at (i)-th and $(i+1)$ ()-th times.

Taking the natural logarithm (ln) of both sides of Eq. (14) gives the logarithm decrement δ as follows:

$$\delta = \frac{\ddot{u}_i}{\ddot{u}_{i+1}} = \frac{2\pi\zeta}{\sqrt{1-\zeta^2}} \tag{15}$$

If ζ is small, $\sqrt{1-\zeta^2} = 1.0$. Hence, Eq. (15) can be expressed by using the following approxi- mation:

$$\delta = 2\pi\zeta \tag{16}$$

For lightly damped systems, the damping ratio can be determined as follows:

$$\zeta = \frac{l}{2\pi} \ln \frac{\ddot{u}_i}{\ddot{u}_{i+1}} \tag{16}$$

In order to obtain the damping ratio with a higher accuracy, it is desirable to relate the ratio of two peaks at several cycles apart, instead of successive two peaks [9]. Over a time period of j cycles apart, the amplitude of the motion decreases from $\ddot{u}_j$ to $\ddot{u}_{j+1}$. This ratio is given by

$$\frac{\ddot{u}_i}{\ddot{u}_{i+1}} = \frac{\ddot{u}_1}{\ddot{u}_2}\frac{\ddot{u}_2}{\ddot{u}_3}\frac{\ddot{u}_3}{\ddot{u}_4} \cdots \frac{\ddot{u}_j}{\ddot{u}_{j+1}} = e^{j\delta} \tag{17}$$

$$\delta = 2\pi\zeta \tag{18}$$

The acceleration time history of the damped free vibration at point 'a' by the heel drop impact is shown in Fig. 14(a) and the response spectrum is presented in Fig. 14(b). The dominant frequency component is 19.04Hz that corresponds to the 1st natural frequency. The acceleration time history and response spectrum of the damped free vibration at point 'b' is shown in Figs. 15(a) and 15(b), respectively. Fig. 15(b) shows the two dominant frequencies of 19.04Hz and 29.79Hz, which are the 1st and 2nd mode frequencies respectively. True damping ratio of the actual floor system can be determined as 1.8% by analyzing Figs. 14 and 15.

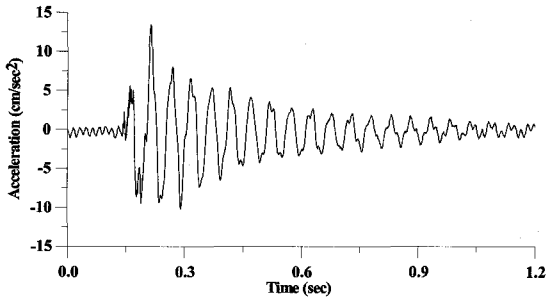

(a) Acceleration response time history of point 'a'

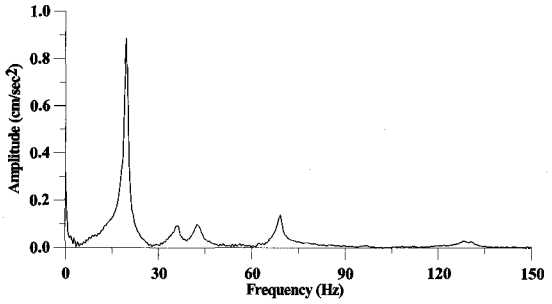

(b) Acceleration response spectrum of point 'a'

〈Fig. 14〉 Acceleration response of point 'a' (peak point of 1st mode shape)

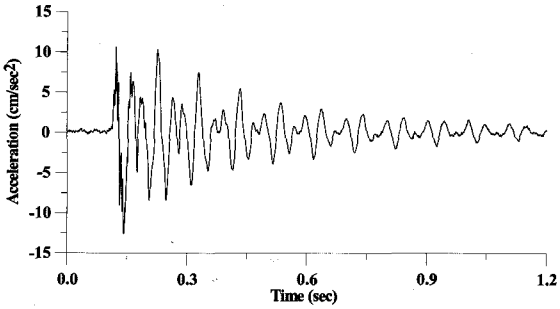

(a) Acceleration response time history of point 'b'

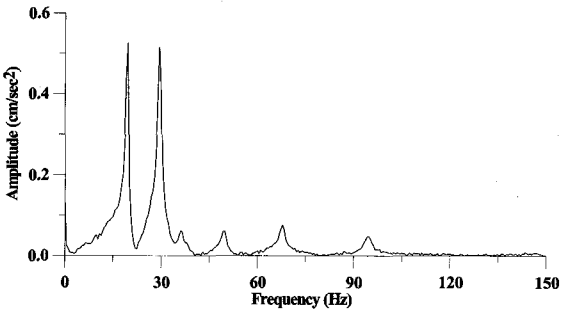

(b) Acceleration response spectrum of point 'b'

〈Fig. 15〉 Acceleration response of point 'b' (antinode of 2nd mode shape)

3.1.2 Response of the actual floor system to heel drop impact

The heel drop impact loads are measured by using the load cell. Theses impact loads are produced when a pedestrian raises his heel and then suddenly drops the heel on the load cell. The load cell is calibrated to zero when the pedestrian steps on the load cell for the elimination of static component from dynamic loads induced by heel drop. The impact load of a pedestrian weighing 64.5kg is shown in Fig. 16. The negative portion of the impact load occurs when the pedestrian raises his heel, because the pedestrian's weight acts on the opposite direction of gravity just before the heel is dropped. As shown in Fig. 16, the impact effect is found to be around 0.3 seconds. The measured heel drop impact loads are very similar to the impact loads presented by Ohmart [11].

The measured responses of point 'a' of the actual floor system subjected to the heel drop impact are compared to the calculated responses by finite element analysis as shown in Fig. 17. Acceleration response of the actual floor system is large due to the effect of impact in the early stage. The damped free vibration response is observed after the impact effect disappears. In general, damping ratio of 3% is applied in the vibration analysis of bare concrete floor systems [8].

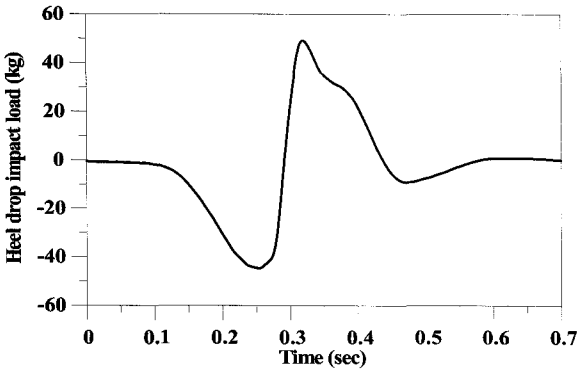

〈Fig. 16〉 Heel drop impact load

However, 3% damping ratio for the actual floor system may not be appropriate due to the reason that the damping ratio of the actual floor system happens to change as a result of cracking and deterioration of the structures. So, it is necessary to determine true damping ratio of actual floor system. The vibration analysis has been conducted by applying the true damping ratio in this study. The acceleration responses of point 'a' obtained from both measurement and analysis are shown in Fig. 26. The measured response is in good agreement with that obtained from the analysis with a damping ratio of 1.8%. Therefore, 1.8% damping ratio is chosen appropriate

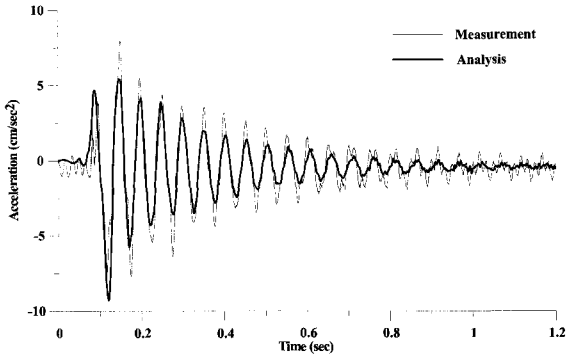

(a) Calculated and measured acceleration response (applying 3.0% damping ratio)

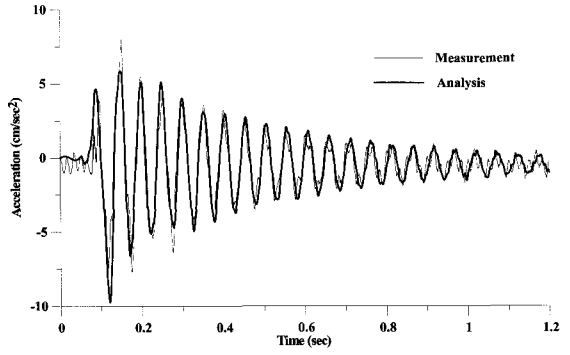

(b) Calculated and measured acceleration response (applying 1.8% damping ratio)

〈Fig. 17〉 Acceleration response of point 'a' of actual floor system induced by heel drop

3.1.3 Response of actual floor system to walking load

The walking loads induced by a pedestrian weighing 78kg walking with the rate of 1.8Hz are applied for the vibration analysis of the actual floor system. Equivalent walking loads of each node are varied according to the size of the plate elements and the location of the foot as shown in Fig. 18(a). The numbers of nodes subjected to the walking loads are represented in Fig. 18(b). Figures 19(a) and 19(b) show the vertical force time history and the y-axis moment time history for each node, respectively

Acceleration responses are measured at point 'a' where the biggest response is expected. The measured response time history is shown in Fig. 20(a) and the calculated response time history is presented in Fig 20(b). Acceleration responses are represented by impulse and periodic shapes because the walking loads are composed of impulse and periodic components. There exists a little difference between the amplitudes of the measured responses and calculated responses, because while the walking loads are applied irregularly in a real situation, the walking loads

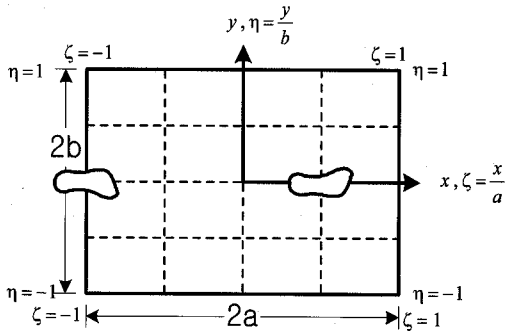

(a) Nodal coordinateof plate element

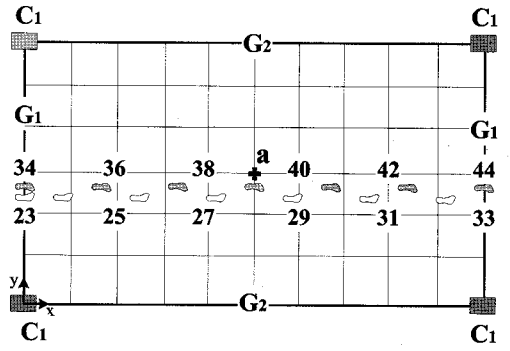

(b) Application of walking loads

〈Fig. 18〉 Application of walking loads to actual floor system

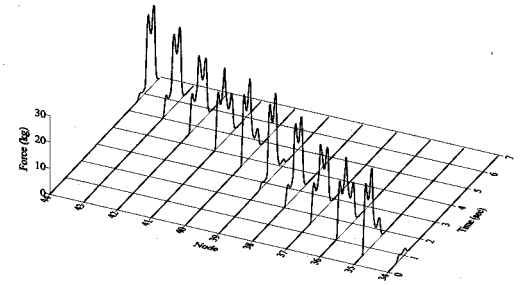

(a) Vertical force - time graphs

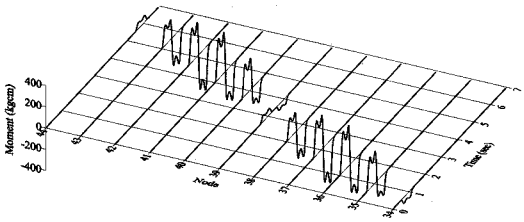

(b) Moment force time graph

〈Fig. 19〉 Equivalent walking loads

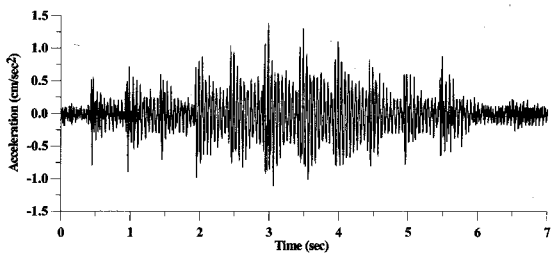

(a) Measured acceleration response of floor system

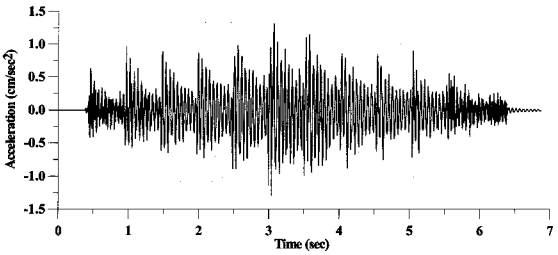

(b) Calculated acceleration response of floor system

〈Fig. 20〉 Acceleration response of point 'a' of actual floor system induced by walking load

in the analytical model are applied regularly. But it is noted that the calculated responses are very similar to the measured responses in the entire response shape. Figure 30 shows the spectrum of the acceleration response. The dominant frequency components occur at the harmonic frequencies of the footsteps. The response spectrum of the measured accelerations is shown in Fig. 21(a). The first peak component takes place at 19.04Hz, the 1st mode frequency. And the other dominant frequency components are 36.38Hz and 43.53Hz corresponding to the 4th and 5th mode frequencies, respectively. Fig. 21(b) represents the response spectrum of accelerations obtained from the vibration analysis. The peak components are represented at the 1st and 5th modes. The amplitudes of the calculated response are smaller than those of the measured responses in the higher frequency range of more than 70.00Hz. But the calculated responses agree well with the measured responses in the entire response shape.

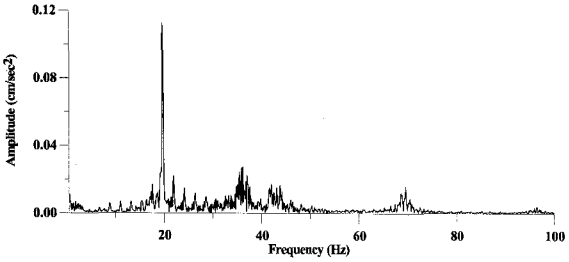

(a) Fourier spectra of measured acceleration response

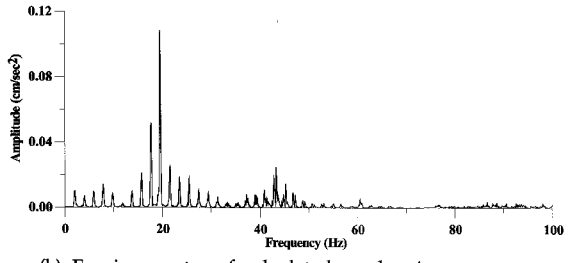

(b) Fourier spectra of calculated acceleration response

〈Fig. 21〉 Fourier spectra of calculated and measured acceleration response of point 'a'

4. Summary and Conclusions

In this study, walking loads are measured directly by using load cells and load time histories induced by walking are analyzed. A new application of walking loads for standard finite element packages is proposed to analyze the floor vibration efficiently. The responses obtained by using the proposed method are quite accurate compared to the measured responses. The results obtained in this study allow the following conclusions to be drawn:

Dynamic load factors of walking loads are largely affected by walking rates. As the walking rates increase, the peak values of dynamic load factors induced by heel strike increase, while the peak values of dynamic load factors produced by toe lift-off and valley points of dynamic load factors decrease. The relationships between these dynamic load factors and walking rates can be used for estimating amplitudes of walking loads.

A series of nodal walking loads with time delays and the equivalent walking loads can be applied for the vibration analysis of structures subjected to walking loads. However, it has a limitation that the walking loads are applied only to nodal points. The method proposed in this study makes it possible to efficiently analyze the vibration of floor systems subjected to walking loads.

This method has been developed for the vibration analysis of floor systems subjected to walking loads, but floor vibrations frequently occur due to other human activities such as jumping, stamping and running. Hence, floor vibration induced by such human activities will be addressed in near future.

5. References

1. Lee D.-G., Kim G.-C.. Modeling of Moving Loads for Analysis of Floor Vibration. Sixth Asian Pacific Conference on Shell and Spatial Structures. Seoul. Korea. 16~18 October 2000;2:869-879
2. Lee D.-G., Ahn S.-K., Kim J.-G.. An Efficient Modeling Technique for Floor-Vibration in Multi-Story Buildings. Structural Engineering and Mechanics 2000; 10(2):603-619
3. Bachmann H, Ammann W. Vibrations in Structures Induced by Man and Machines. Structural Engineering Documents 3e. IABSE. 1987.
4. Weaver W, Johnston PR. Finite Elements for Structural Analysis. New Jersey: Prentice Hall. 1984.
5. Ellingwood B, Tallin A. Structural Serviceability: Floor Vibrations. Journal of Structural Engineering Division, ASEC 1984; 110(2):401-417.
6. Mouring SE, Ellingwood B. Guideline to Minimize Floor Vibrations from Building Occupant. Journal of Structural Engineering Division, ASEC 1994;120(2) :507-525.
7. Wu JJ, Whittaker AR. The Use of Finite Element Techniques for Calculating The Dynamic Response of Structures to Moving Loads. Computers and Structures 2000; 78(2):789-799.
8. Steel Structures for Buildings Proposed Appendix G. Standard S16-69. Canadian Standards Association. Ontario.
9. Chopra AK. Dynamics of Structures. New Jersey: Prentice Hall, 1995.]
10. Kim G.C., Lee D.G.. Modeling of Walking Loads for Floor Vibration Analysis. COSEIK 2002;15(1):173-187.
11. Ohmart RD. An Approximate Method for The Response of Stiffened Plates to A Periodic Excitation on Studies in Engineer- ing Mechanics. Report No. 30. The University of Kansas. Center for Research in Engineering Science. Lawrence. Kansas. April 1968.